Journal of Atmospheric and Solar–Terrestrial Physics 229 (2022) 105834

Contents lists available at ScienceDirect

Journal of Atmospheric and Solar-Terrestrial Physics

journal homepage: www.elsevier.com/locate/jastp

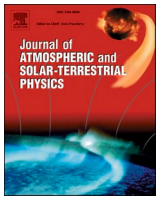

Research Paper

Earthquakes associated subionospheric VLF anomalies recorded at two low latitude stations in the South Pacific region

Sarwan Kumar, Sushil Kumar *, Abhikesh Kumar

School of Information Technology, Engineering, Mathematics and Physics (STEMP), The University of the South Pacific, Fiji

ARTICLE INFO

Keywords:
VLF perturbations
D-region
Earthquakes
Atmospheric gravity waves
Wavelet analysis

ABSTRACT

The JJI VLF (22.2 kHz) transmitter signal received at two low-latitude stations, one in Port Vila (geog. coord., 17.73°S, 168.33°E), Vanuatu and other in Suva (18.14°S, 178.44°E), Fiji, was analyzed for any VLF changes due to 16 Earthquakes (EQs) with magnitudes 5.5 to 7.7, during 2018 (JJI-Vanuatu path, 6.8 Mm) and 2007 to 2018 (JJI-Suva path, 7.5 Mm). The VLF signal amplitude analysis included terminator time (TT), average daytime and nighttime amplitude variation, nighttime fluctuation, and mother Morlet wavelet methods. Out of 16 EQs only eleven EQs have shown subionospheric VLF changes including the decrease in the amplitude for about 2–8 h on the EQ day, unusual shifts in the TT of up to 5–9 min, and the decrease in the average daytime and nighttime signal amplitude of about 1–1.5 dB and 1–5 dB, respectively, on the mainshock day of the EQs. The $dA(t) < 0$ condition was observed about 4–5 days before the EQ which stabilized after 3–4 days from the EQ day. A decrease in the non-normalized and normalized trend of below -2σ (standard deviation) mark was found on the EQ day and an increase in the non-normalized and normalized NF and dispersion of above +2σ mark on the day of seismic activity was found. Mother wavelet analysis of EQ associated changes in the signal amplitude showed a strong and enhanced presence of short frequency (~0.05–0.10 mHz) wave-like signatures, a few days prior, on the day of EQ, and after the EQ day as compared to normal days.

1. Introduction

Earthquakes (EQs) occur as an alarming catastrophe, posing danger to the infrastructure and human life. The ability to precisely predict EQs will indeed help prevent substantial loss of life, assets, ecosystem and environment. The study of lithosphere-atmosphere-ionosphere coupling is primarily focused on the comprehension and analysis of ionospheric anomalies initiated by the lithospheric activities (Pulinets and Ouzounov, 2011). EQs are known to be the source of atmosphere-ionosphere anomalies because of the surface ionization from the radioactive decay of radon emanations (Silva et al., 2013) and the generation of geo-electric charges (Freund, 2013) which can propagate through the atmosphere triggering the ionospheric electric field perturbations (Silva et al., 2011) and thermal anomalies (Kakinami et al., 2013). Eventually, they can disturb the lower ionosphere which can be sensed by the Extremely Low Frequency (ELF), Very Low Frequency (VLF) and Low Frequency (LF) emissions (Němec et al., 2008; Righetti et al., 2012). Further mechanisms support the generation of acoustic pressure waves (Astafyeva et al., 2013), discharge of positive holes (Freund, 2013), and underground release of aerosols (Pulinets et al., 2000).

VLF (3–30 kHz) navigational transmitter signals have the potential to be used as one of the means to detect the lower ionospheric signatures of EQs. Most of the energy emitted by the VLF/LF transmitters is trapped between the earth's surface and the lower ionosphere, forming the earth-ionosphere waveguide (EIWG). Due to low attenuation at long wavelengths, VLF signals can travel long distances by multiple reflections in the EIWG. Many researchers have presented their work on the perturbations of the ionospheric D-region due to changes in the propagation conditions for VLF signals before the EQ day (Hayakawa et al., 2011; Nina et al., 2021). However, there is no clear consensus in the scientific community on the lower ionospheric perturbations associated with EQs and further investigations using the larger data set are warranted. There are many other terrestrial and space weather phenomena that might influence the VLF signals, for example, the ionosphere is greatly influenced from above by the solar flares and geomagnetic storms (e.g., Kerrache et al., 2021; Kumar et al., 2015; Selvakumaran et al., 2015) and from below by the thunderstorms and tropical cyclones (TCs) (Kumar et al., 2017; Rodger, 2003; Salut et al.,

* Corresponding author.
E-mail addresses: sarwankumar414@gmail.com (S. Kumar), kumar_su@usp.ac.fj (S. Kumar), abhikesh.kumar@usp.ac.fj (A. Kumar).

https://doi.org/10.1016/j.jastp.2022.105834
Received 17 November 2021; Received in revised form 22 January 2022; Accepted 24 January 2022
Available online 31 January 2022

2012, 2013).

The quest for pre-seismic ionospheric signatures has always been argumentative. Some of the previous documents have reported unanticipated and infrequent changes in the atmospheric and ionospheric parameters before a seismic activity. The present work deals with ionospheric precursory signatures of 16 seismic events that occurred near the JJI paths to a low-latitude station located in Port Vila, Vanuatu and a station in Suva, Fiji, over the transmitter-receiver great circle paths of length 6.8 Mm and 7.5 Mm, respectively. The JJI amplitude data have been analyzed for both paths to examine any effect of the EQs. 7 EQs occurred along JJI to Vanuatu path while 9 along JJI to Fiji path. We have considered the EQs that had shallow-focus (less than 70 km) and mid-focus (70–300 km) with a magnitude of more than 5.5 on the Richter scale. The epicenters of 10 EQs were located within the fifth Fresnel zone (wave sensitive area) to the propagation path. The Fresnel zone is an elliptical area (ellipsoid boundaries with foci at the transmitter and the receiver) around the visual line-of-sight that radio waves spread out into from the VLF transmitter to the receiver. The fifth Fresnel zone is defined as the locus of points in 3D space such that two segment path from the transmitter to the receiver that deflects off a point on that surface will be between 4^{th} and 5^{th} half-wavelength out of phase with the straight-line path. The detailed analysis for two EQs has been presented as case studies (M6.0 on December 14, 2016 and M7.5 on December 5, 2018) results of which along with other 14 EQs have been summarized in Table 1. The anomalies in the VLF signal due to EQs are then justified by eliminating the effects of the strong thunderstorms, TCs, geomagnetic storms and solar flares which can also produce VLF anomalies (Kumar et al., 2013).

2. Methodology

Subionospheric VLF signal from Japan (JJI, geographical location 32.05°N, 130.83°E) operating at 22.2 kHz, was recorded at Suva (geographical location 18.14°S, 178.44°E), Fiji, and Port Vila (geographical location 17.73°S, 168.33°E), Vanuatu, VLF stations by using SoftPAL. SoftPAL (software based amplitude and phase logger) can record narrowband VLF data at up to 10 ms resolution from 7 MSK transmitters at a time. Locations of the VLF transmitter, the receivers at Suva and Port Vila, and the transmitter-receiver great circle paths (TRGCPs) are illustrated in Fig. 1. The VLF amplitude data from March to December 2018 were used to examine the EQs effect in the JJI transmitter signal to Port Vila path and during 2007–2018 amplitude data (excluding the data for 2017 and the first few months from the year 2018) to Suva. One-minute average values obtained from 0.1s resolution recording have been used. The occurrence of EQs along the TRGCPs was tracked from the Earthquake Track, Today's Earthquake in Fiji (https://earthquaketrack.com/r/fiji/recent). The *Dst* and *Kp* indices were retrieved from the World Data Center (WDC) Geomagnetic data Services, Kyoto, Japan (http://wdc.kugi.kyoto-u.ac.jp/wdc/Sec3.html).

Occurrence of the EQs near JJI-Suva and Vanuatu TRGCPs were within and beyond the wave sensitive zone (fifth Fresnel zone) as shown in Fig. 1. The diurnal variation in the signal amplitude, terminator time (TT), nighttime and daytime average amplitude, nighttime fluctuation (NF), and mother Morlet wavelet methods have been used for VLF amplitude data analysis. TT is defined as the time where the minima occur in the received VLF signal amplitude or step changes in the phase during the transition of the day-night terminator between the

Table 1
List of the earthquakes that occurred along the JJI to Port Vila, Vanuatu and Suva, Fiji GCPs with any effect on the JJI signal.

No.	Earthquake information					Distance from the TRGCP path (km)	Effect on VLF signal
	Date	Event time	Location	M_w	Depth		
	YY/M/D	(UT hours)			(km)		
1	2007/10/06	13:38	Mariana Islands	6.1	20	90.7	Variation in VLF signal, average nighttime amplitude, enhanced NF, and wavelet fluctuations were noticed
2	2008/05/09	21:51	181.2 km from Merizo Village, Merizo, Guam	6.8	76	690.6	A minor effect in VLF signal, change in average nighttime and daytime amplitude, NF, and wavelet fluctuations were noticed
3	2012/07/06	02:28	51.2 km from Port-Olry, Sanma, Vanuatu	6.3	160	638.0	No effect
4	2012/10/20	23:00	112.2 km from Sola, Torba, Vanuatu	6.2	36	623.5	Effects on VLF signal, and NF and wavelet fluctuations were noticed
5	2012/11/17	02:51	42.2 km from Port-Olry, Sanma, Vanuatu	5.6	123	651.8	No effect ($Dst = -108$ nT on 2012/11/14)
6	2016/07/29	21:18	366.2 km from Saipan, Saipan, Northern Mariana Islands	7.7	212	51.0	Effects on average nighttime amplitude, and NF were noticed
7	2016/12/14	02:21	Mariana Islands	6.0, 5.5	27, 31	74.9	Perturbations in VLF signal, nighttime amplitude changes, NF, and wavelet fluctuations were observed
8	2016/12/21	16:43	Mariana Islands	5.9	16	165.8	Signal power decreased
9	2018/03/29	18:51	42.2 km from Honiara, Guadalcanal, Solomon Islands	5.8	32	244.1	Variation in the VLF signal, average nighttime amplitude, and enhanced NF were noticed
10	2018/08/21	22:32	79.2 km from Lakatoro, Malampa, Vanuatu	6.5	13	668.1	Effects on average nighttime and daytime amplitude, and NF and wavelet fluctuations were noticed
11	2018/09/18	11:57	48.2 km from Gizo, Western Province, Solomon Islands	5.8	10	392.4	No effect
12	2018/09/20	05:47	169.2 km from Buala, Isabel, Solomon Islands	5.5	10	334.4	No effect
13	2018/11/16	03:26	132.2 km from Kirakira, Makira, Solomon Islands	6.2	10	5.7	Shift in TT, slight change in average nighttime amplitude, and effect on NF and dispersion were noticed
14	2018/12/05	04:18	168.2 km from Tadine, Loyalty Islands, New Caledonia (M7.5)	6.0, 7.5, 5.9, 5.6, 5.7	10	183.4	Shift in TT, effects on VLF signal, average nighttime and daytime amplitude, NF, and wavelet fluctuation were noticed
15	2018/12/15	20:21	90.2 km from Lakatoro, Malampa, Vanuatu	5.6	34	79.3	A minor effect in VLF signal, shift in TT, and wavelet fluctuation was noticed
16	2018/12/22	14:25	105.2 km from Sola, Torba, Vanuatu	6.0	42	142.6	Nighttime and daytime amplitude changes, and NF were noticed

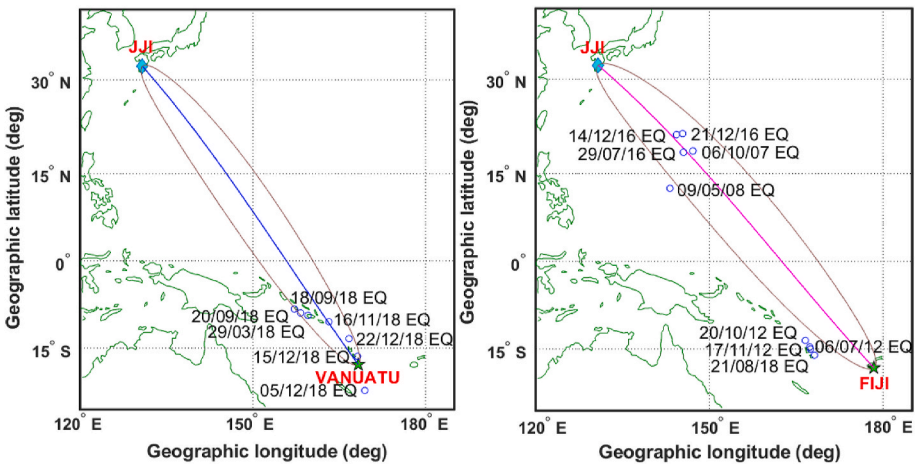

Fig. 1. The great circle path between the JJI VLF transmitter, Japan, and the two receiving stations; Port Vila, Vanuatu (left) and Suva, Fiji (right). The wave sensitive area defined by the fifth Fresnel zone is plotted with the brown ellipse. The 7 earthquake epicenters in the JJI to Vanuatu path (left) and 9 earthquake epicenters in the JJI to Suva path (right) are marked with the blue circle. (For interpretation of the references to color in this figure legend, the reader is referred to the Web version of this article)

transmitter and the receiving station. For the diurnal variation in the signal amplitude of the JJI to Suva, Fiji and Port Vila, Vanuatu TRGCPs, signal amplitude over-plotting of seven days prior (-7 d) and seven days after (+7 d) the EQ day was done. Under the TT method, the occurrence of sunrise and sunset amplitude minima was examined seven days before and seven days after the EQ main shock. Only sunrise minima were examined because the sunset minima were not identifiable for most of the time and during the daytime JJI transmitter was at times off-air. The phase data have not been used as JJI is a phase unstable transmitter. For daytime and nighttime average amplitude analysis, the daytime is when the TRGCP is in the complete light and the nighttime is when the TRGCP is in complete darkness. Under the NF method, the fluctuations in the nighttime average signal amplitude were obtained using:

$$dA(t) = A(t) - A_{av}(t) \quad (1)$$

where $dA(t)$ is the difference between signal amplitude and the standard average at a particular time t. $A(t)$ is the VLF signal amplitude at a particular time t during the night, and $A_{av}(t)$ is the standard average amplitude over ±7 days at a particular time t. The $dA(t)$ area plot displays the fluctuation level for the seismo-ionospheric effect. The quantity $dA(t) < 0$ is the only important element for the seismogenic effect because mean nighttime amplitude decreases around the EQ day (Hayakawa et al., 2011). This method is further divided into other statistical quantities such as trend (T), nighttime fluctuation level (NF), dispersion (D), and their respective normalized quantities. The trend is the average of nighttime $dA(t)$ values for each day and the normalized trend is calculated using the formula:

$$T^* = (trend - < trend >)/\sigma_T \quad (2)$$

where $<trend>$ is the average trend for ±7 days around the EQ day, and σ_T is the standard deviation of the trend for the designated days. The NF is the integral of $[dA(t)]^2$ values over the individual nighttime hours. Dispersion (D) is the standard deviation of $dA(t)$ values for each day. The normalized nighttime fluctuation (NF*) and normalized Dispersion (D*) are calculated in a similar way to the normalized trend, T* (Hayakawa et al., 2010).

Also, we have applied the mother Morlet wavelet technique (Mallat, 1999) to the JJI signal amplitude during the disturbed period to estimate if there are any wave-like signatures (WLS) present in the JJI VLF signal due to EQ-associated gravity waves. We have estimated the nighttime JJI signal amplitude perturbation for each day by finding the amplitude difference between ±7 days average and respective EQ days.

3. Results

JJI transmitter signal propagates across the geomagnetic equator over the ocean mainly in the north to south direction with small component in the west to the east direction to Port Vila, Vanuatu and Suva, Fiji. A total of 16 EQs with magnitude ranging from 5.5 to 7.7 at 10–212 km depth were analyzed for any subionospheric VLF anomalies in the JJI signal received at both the stations. The effects of 7 EQs were seen for JJI to Vanuatu path while 9 EQs for JJI to Fiji path. The epicenters of 10 EQs were located within the fifth Fresnel zone (wave sensitive area) to the propagation paths while 6 EQs occurred slightly beyond the fifth Fresnel zone. The reason for including these 6 EQs is because recent research has shown that perturbations in the VLF signal amplitude can also occur due to EQs with the epicenter located outside the fifth Fresnel zone (Phanikumar et al., 2018). Table 1 shows details of these EQs for each transmitter-receiver path including the date, time and place of occurrence, the seismic magnitude as measured from the Richter scale, depth of the EQ, the EQ distance from the JJI-Vanuatu/Suva great circle paths (GCPs), and any effect observed on the VLF propagation. Out of 11 EQs that showed VLF effects, the detailed analysis for only 2 EQs which occurred on December 14, 2016 in the JJI-Fiji GCP and December 5, 2018 in the JJI-Vanuatu GCP, are presented as case studies and analysis for other EQs is summarized in Table 1.

3.1. JJI to suva VLF signal analysis: December 14, 2016 earthquake

An EQ of magnitude 6.0 occurred on December 14, 2016 at Mariana Islands (21.2° N, 144.4° E). The EQ had a shallow epicenter at 27 km depth and occurred 74.9 km away from JJI-Suva GCP (EQ epicenter located within the fifth Fresnel zone). An overplot of diurnal variation in the signal amplitude to Suva, Fiji, GCP, for seven days prior (-7 d) and five days after (+5 d) the EQ from 14 December is shown in Fig. 2a. The local time of Fiji is LT = UT + 12 h. During 23-07 UT, the data are excluded from each day due to the transmitter being off-air. The red line plot (EQ day) in panel (a) shows the signal amplitude on a seismic day (0–23 UT hours) as recorded by SoftPAL. During the EQ day, approximately for more than 2 h (about 15–17 UT) at the nighttime, the signal amplitude decreased (~6.9 dB at 16:33 UT) before the sunrise transition. To verify that the anomalies observed were due to this seismo-ionospheric event and were not caused by extreme tropical weather events such as the TCs (there were no TCs active during this EQ) and extreme space weather events (e.g., geomagnetic storms and solar flares), the *Dst* and *Kp* indices (http://wdc.kugi.kyoto-u.ac.jp/wdc/Sec3.html) for a few days prior and after the seismic event were plotted. Panel (b) showing the variation in the *Dst* and *Kp* indices clearly indicates no significant geomagnetic activity (decrease in the *Dst* index below −50 nT and increase in *Kp* index exceeding 5). There were no TCs nearby the EQ occurrence region on the anomalous day (14 December).

Fig. 3 shows the stacked diurnal variation in the JJI signal amplitude

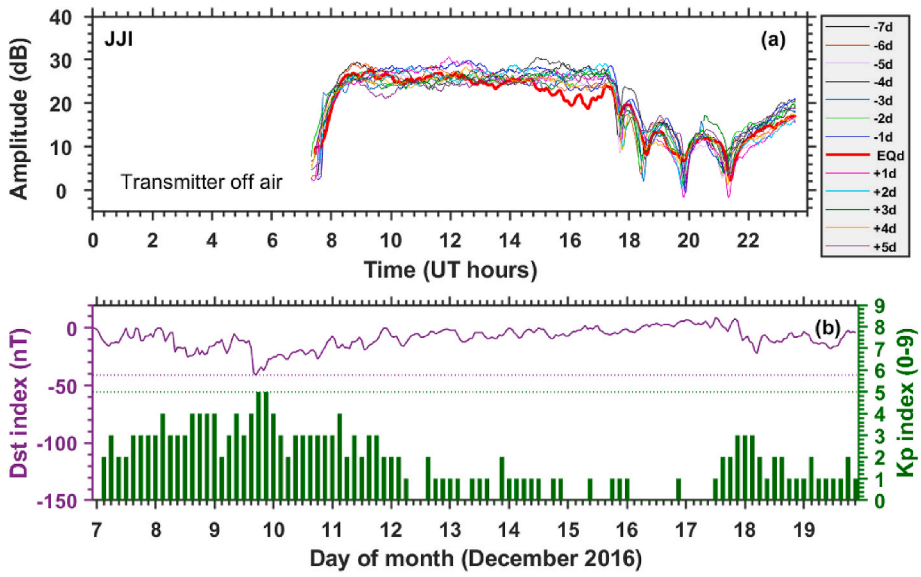

Fig. 2. (a) Diurnal variation in the signal amplitude of the JJI to Suva, Fiji, GCP for seven days prior and five days after the earthquake on December 14, 2016 with a magnitude of 6.0 and a focus depth of 27 km and (b) variation in the *Dst* and *Kp* indices for the days prior to and after the earthquake.

to Suva, Fiji, during 7–19 December 2016. The dashed vertical lines during the sunrise minima (SR_1, SR_2, SR_3, and SR_4) are used to identify any shift in the TTs. The amplitude data during daytime and sunset transition have been removed due to low signal strength/transmitter off-air, therefore, no analysis has been carried out for the sunset terminator. The diurnal amplitude variation from 09 to 17 UT corresponds to propagation over complete darkness. The times at which minima in the received signal amplitude (sunrise/sunset transition) occur are the measures of TTs during passage of sunrise and sunset terminator between the transmitter and receiver or vice-versa. On the normal days in absence of EQs, TTs are considered to be fairly consistent from day to day. The sunrise minima times were analyzed for 15 days, but the TT results are shown 7 days prior and 5 days after the seismic event due to the limitation of diurnal data availability in December. There was no apparent anomaly detected during sunrise minima due to the 14 December EQ, however, SR_1, SR_3, and SR_4 minima shifted gradually due to daily variation and SR_2 minima diminished after the EQ day.

The mean signal amplitude at the nighttime (09–17 UT hour) for the JJI to Suva, Fiji, propagation during 7–19 December is plotted in Fig. 4. The average daytime amplitude data has not been analyzed due to a very low daytime signal strength because of the transmitter being off-air. The red arrow (Fig. 4) on 14 December indicates the EQ day. It can be seen that the average nighttime signal changes randomly but a significant decrease (minimum) in the nighttime signal strength was observed (around 23.9 dB) on the EQ day (14 Dec). The minimum average nighttime signal on the days (7–19 December) other than EQ day was more than 24.9 dB. The reduced signal strength is due to higher attenuation to VLF propagation in the EIWG because attenuation depends on the reflection height of the VLF signal, where the higher attenuation is offered by EIWG with reduced D-region height (Kumar et al., 2008). The decreased signal strength indicates a decrease in the VLF reflection height.

A statistical analysis of nighttime fluctuation (NF) of the signal amplitude was carried out to verify if any perturbations that occurred at the nighttime during the period of EQ activity were associated with EQ, as reported by several researchers (Hayakawa et al., 2011; Kasahara et al., 2010; Kumar et al., 2013). The NF analysis for 7–19 December for the JJI to Suva, Fiji, GCP is shown in Fig. 5. The solid horizontal line ($y = 0$ line) in each panel represents the average nighttime amplitude. At any time it rises or falls above an average value, the $dA(t)$ values are represented by the red shaded region. The blue dashed ellipse on 14 December (EQ day) indicates an increase in the occurrence of $dA(t) < 0$ condition, typical of an EQ effect.

Statistical analysis of the trend (T), NF, dispersion (D), and their respective normalized quantities of the VLF signal has been carried out, where the signal anomaly is considered by the simultaneous drop in the T and rise in the NF and D (Hayakawa et al., 2010; Kumar et al., 2013). Fig. 6 shows the graphical representations of the T (a), NF (c), and D (e) in each panel (left) during 7–19 December for the JJI-Suva, Fiji, GCP. The panels (b, d and f) on the right side represent normalized values of the T, NF, and D. To make analysis easier to understand, the blue horizontal dashed guidelines showing the $\pm 2\sigma$ levels have been drawn. The red solid circle on the columns indicates anomalous signal amplitude (crossing the horizontal 2σ lines) due to the EQ. Similarly, the corresponding thresholds for NF and D are given by $+2\sigma$ (same color) horizontal line. The trend values decreased and touched the -2σ line on 14 December for both non-normalized and normalized panels (Fig. 6a and b). The NF was enhanced two days before the EQ and passed the $+2\sigma$ line on the day of the EQ in both non-normalized and normalized panels (Fig. 6c and d). The NF began to rise from 12 December to 14 December and slowly decreased before crossing the $+2\sigma$ line on the EQ day. The normalized D showed a similar pattern as non-normalized D.

Fig. 7 shows the Morlet wavelet analysis of JJI signal to Suva, Fiji, VLF signal amplitude perturbations at the nighttime (11–17 UT) of TRGCP for the period 7–19 December. The *x*-axis represents the day of the month while the *y*-axis shows the frequency ranging from 0.05 to 0.45 mHz. The sunset/sunrise and day time period have been excluded because the strong sunrise/sunset terminator effect dominates the EQ associated wave-like signatures and at times transmitter goes off-air in the daytime. At the nighttime, the wavelet spectra of a short frequency between 0.05 and 0.10 mHz with enhanced strength were observed during 14–15 December.

3.2. JJI to Port Vila VLF signal analysis: December 5, 2018 earthquake

An EQ at the location 21.9° S, 169.4° E (168.2 km from Tadine, Loyalty Islands, New Caledonia) occurred on December 5, 2018 with a magnitude of 7.5 and at a shallow depth of 10 km at a distance of 183.4 km from the JJI-Port Vila GCP. This EQ occurred beyond the fifth Fresnel zone. The diurnal variation in the signal amplitude for six days prior and seven days after the EQ is presented in Fig. 8a. The local time of Vanuatu is LT = UT + 11 h. A decrease in the nighttime signal

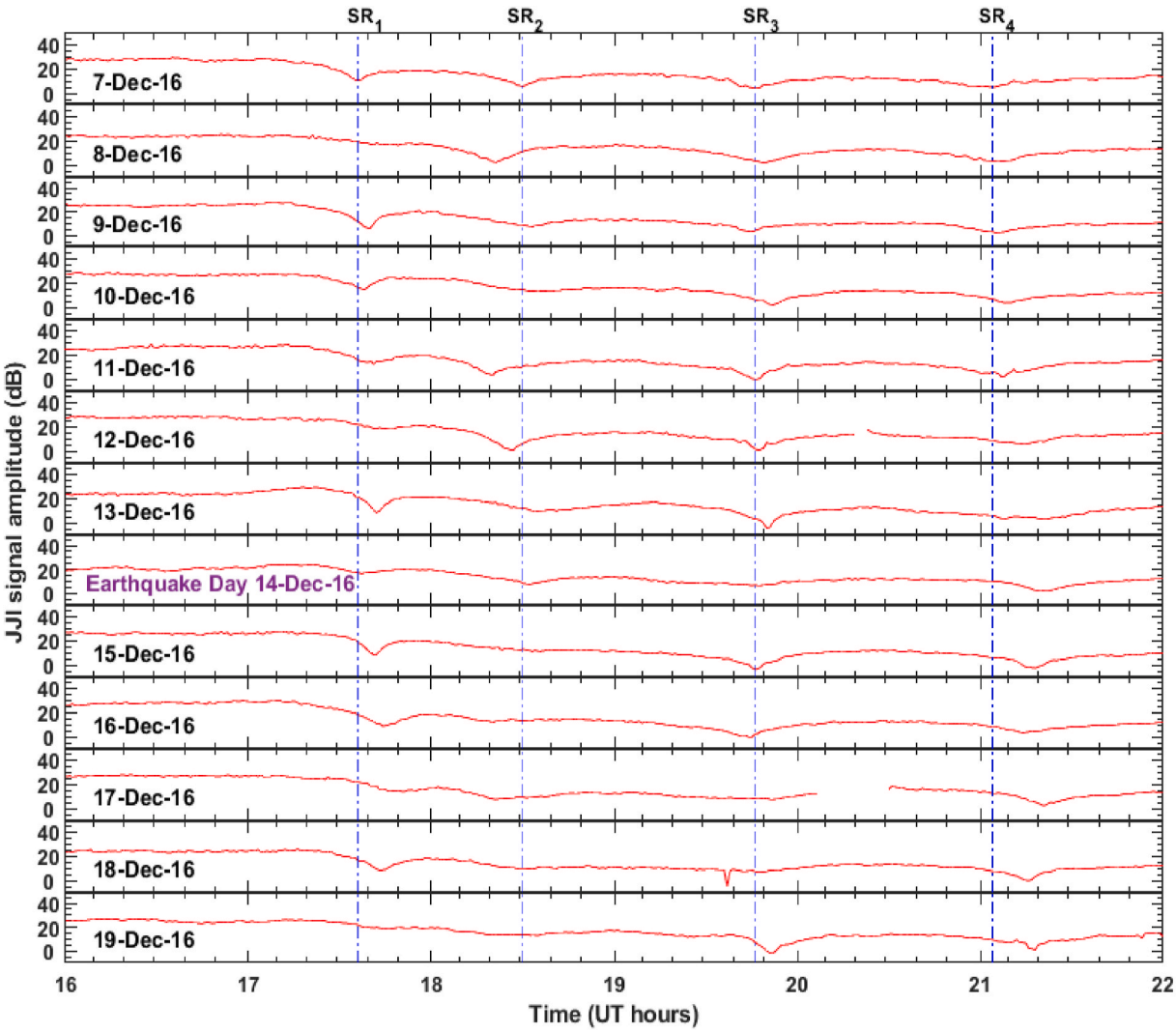

Fig. 3. Diurnal variation in the signal amplitude of the JJI to Suva, Fiji, during the period of 7–19 December 2016 associated with the earthquake on 14 December with a magnitude of 6.0 and a focus depth of 27 km. The horizontal axis represents time in UT while the vertical axis in each panel shows the signal amplitude (dB). The dashed vertical lines on the sunrise minima (SR_1, SR_2, SR_3, and SR_4) indicate shift in the terminator times.

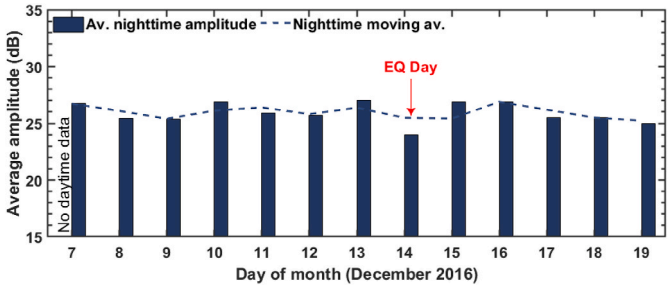

Fig. 4. The average amplitude at the nighttime (09–17 UT hours) of JJI signal for Suva, Fiji, path for a period of 7–19 December 2016. The red arrow on the 14 December indicates the earthquake day. (For interpretation of the references to color in this figure legend, the reader is referred to the Web version of this article)

amplitude was observed over 8 h starting from 10 UT to 18 UT on the EQ day. The plot of the *Dst* and *Kp* indices in Fig. 8b shows no significant decrease in *Dst* index and increase in *Kp* index, indicating this as a magnetically quiet period. There was no TC nearby EQ occurrence region on the EQ day (December 5, 2018). The amplitude remained low for most of the time during the nighttime hours on 5 December (red solid line) compared to other days as can be seen from the diurnal plots in Fig. 8a.

Fig. 9 shows diurnal variation of the JJI signal amplitude from 16 to 22 UT at Port Vila, Vanuatu, during 29 November to 12 December associated with the December 5, 2018 EQ. The dashed vertical line on the sunrise minima (SR_1) indicates any shift(s) in the TTs. The signal during the sunset terminator was not analyzed because of the instability of the JJI-Vanuatu signal during sunset transition and later during sunrise (excluding SR_1 minima). The average shift for the 14 days in the occurrence times of these minima was found ~4 min. The shift of sunrise minima time was 5 min toward the right as shown in the panel indicating as if the nighttime hours have slightly been prolonged. After the EQ event, the minima started to recover from the shifted position and finally settled to the pre-event time on 10 December.

Fig. 10 shows the average daytime and nighttime amplitude (dB) over 14 days from EQ day for the JJI to Port Vila, Vanuatu, path. It can be seen that the average nighttime signal strength started to decrease on 4 December and became minimum on 5 December (43.1 dB) and then increased after the EQ day. Concerning 3 December (reference day), the average amplitude on EQ day was reduced by 5.3 dB. The average daytime signal strength started to decrease from 5 December, attaining minimum signal strength on 8 December (36.5 dB) and then recovered.

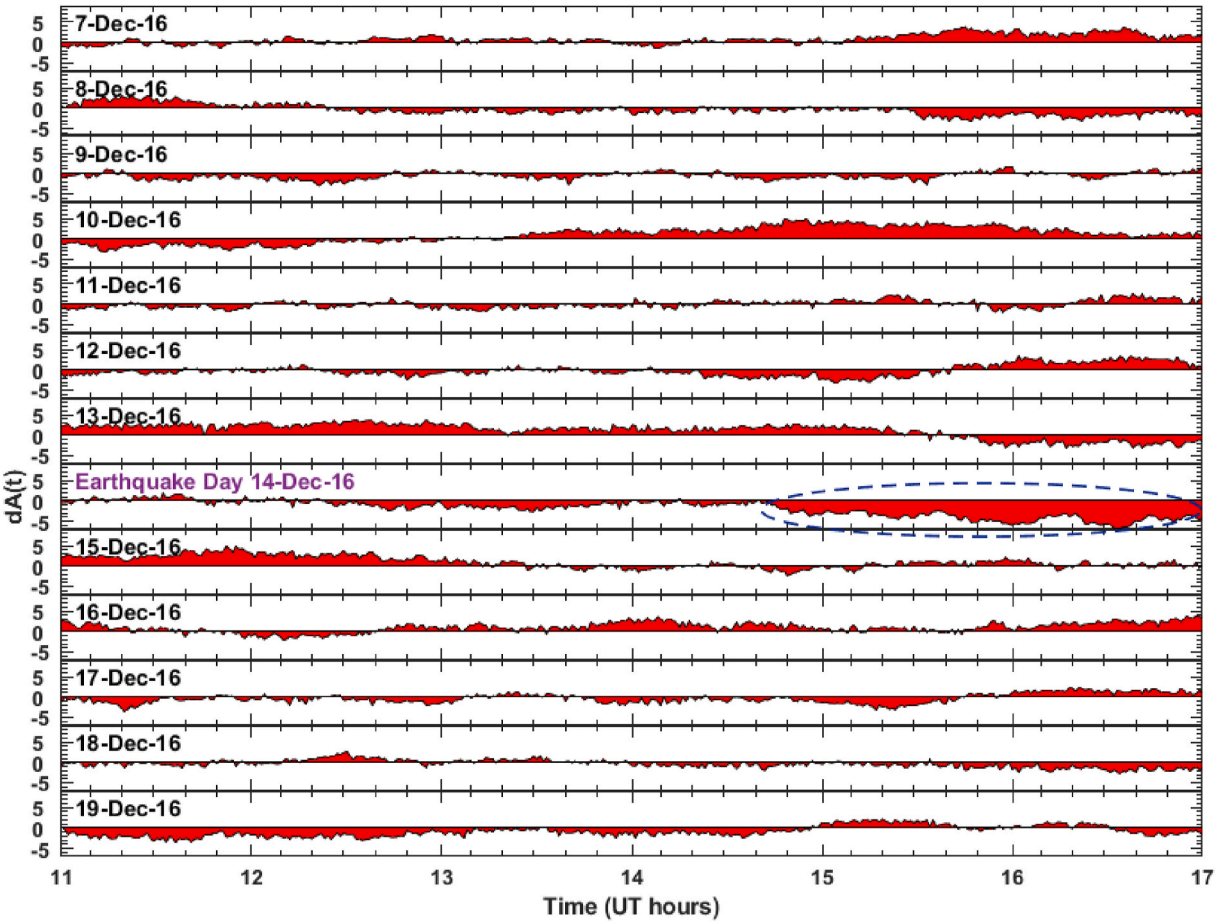

Fig. 5. Fluctuations in the nighttime signal strength (*y*-axis in dB) during 7–19 December 2016 for the JJI to Suva, Fiji, GCP. The blue dashed ellipse indicates an increase in the occurrence of $dA(t) < 0$ conditions on the earthquake day. (For interpretation of the references to color in this figure legend, the reader is referred to the Web version of this article)

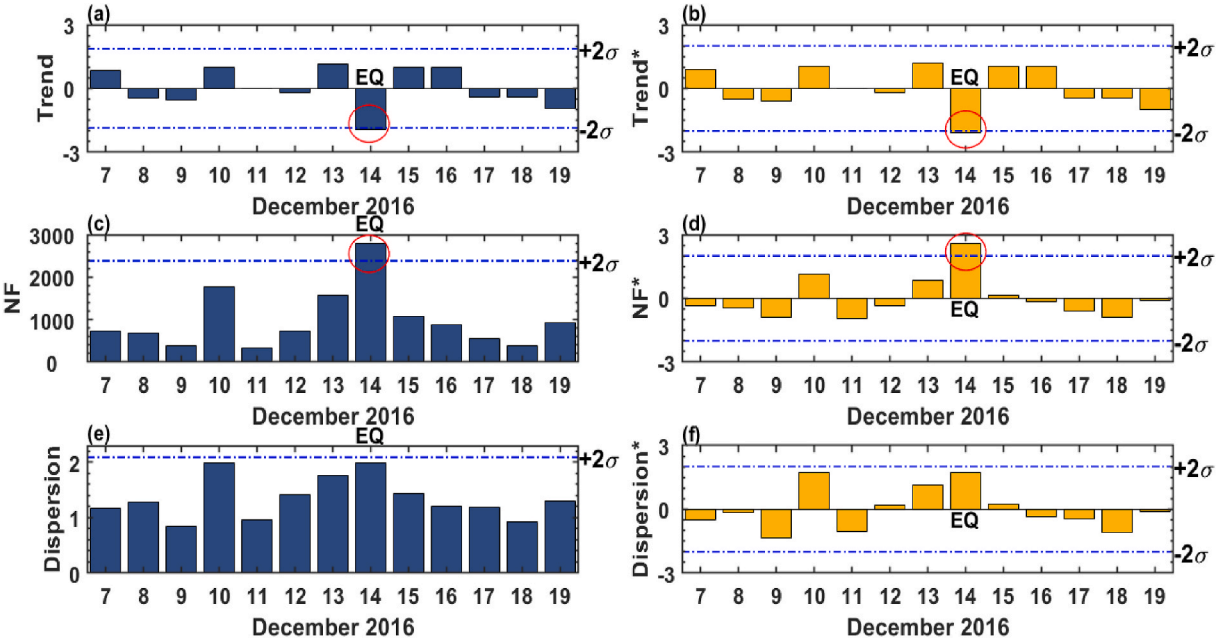

Fig. 6. Graphical representation of the trend (a), nighttime fluctuation (c), and dispersion (e) in each panel (left) during the period 7–19 December 2016 for the JJI signal to Suva, Fiji, GCP. The panels (b, d and f) on the right side represent normalized values of the trend, NF, and dispersion. The blue horizontal dashed lines shows the $\pm 2\sigma$ criterion. The red circle on the columns indicates anomalous values (crossing the 2σ lines). (For interpretation of the references to color in this figure legend, the reader is referred to the Web version of this article)

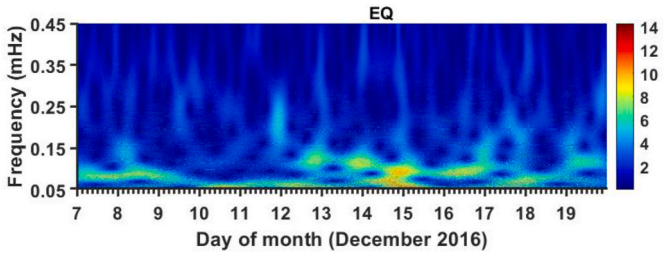

Fig. 7. The wavelet spectra of JJI VLF signal received at Suva, Fiji, at the nighttime (11–17 UT hours) for the period 7–19 December 2016. The earthquake day is 14 December.

On 5 December, the average nighttime amplitude was recorded 39.9 dB giving a reduction of 3.5 dB on 8 December as compared to 5 December. The nighttime $dA(t)$ values during 29 November to 12 December for the JJI to Port Vila, Vanuatu, GCP are shown in Fig. 11. The figure reveals an increase in $dA(t) < 0$ conditions between 1–9 December which reduced after 9 December. The NF started to decrease 4 days before the EQ and stabilized after the 4th day of the EQ.

Fig. 12 shows the graphical representation of the T (a), NF (c), and D (e) in each panel (left) during 29 November to December 12, 2018 for the JJI to Port Vila, Vanuatu GCP. The panels (b, d and f) on the right side represent normalized values of the T, NF, and D. The T value touched the -2σ line on 5 December (EQ day) in both non-normalized and normalized panels (Fig. 12a and b). The NF exceeded the +2σ line on the day of the EQ in both non-normalized and normalized panels (Fig. 12c and d). The NF did not exceed the +2σ line, however, it increased before and after the EQ day (1st, 3rd, 7th, and 8th December). The normalized D showed a similar pattern as non-normalized D. In Fig. 13, the Morlet wavelet analysis of nighttime (09–17 UT) VLF signal perturbations from 29 November to December 12, 2018 shows an intense wavelet signal of 0.05–0.08 mHz on 7 and 8 December 2018.

4. Discussion

A significant amount of research has been done on the ionospheric seismic effect, however, there is no clear consensus on the ionospheric response to seismic phenomena and for any tangible ground for forecasting EQs based on the ionospheric response. Noticeable progress has been made on interconnectivity in the lithosphere-atmosphere-ionosphere (LAI) system but still needs further comprehensive data analysis particularly on the D-region response to seismic activities. In this work, anomalies in the VLF signal propagation were determined to find if the lower ionosphere can be perturbed by the EQ events. The anomalies were observed for 11 out of 16 EQs occurring within and slightly beyond the wave sensitive region (fifth Fresnel Zone) with a magnitude greater than 5.5 and at the shallow-focus and mid-focus depths. However, there exist many other factors apart from EQs which might influence the VLF propagation, for example, solar flares, geomagnetic storms, thunderstorms, cosmic and gamma rays flashes, and direct or indirect effects of lightning. Any effects of these phenomena were identified and removed as we know the occurrence time and duration of each of these events.

Out of 16 EQs, 4 EQs on May 9, 2008, 29 March, 21 August and November 16, 2018 occurred during the TCs and three of them showed EQ like anomalies in the VLF signal, and an EQ on November 17, 2012 occurred after an intense geomagnetic storm on November 14, 2012 ($Dst = -108$ nT) which did not show any anomaly in JJI signal. Fig. 14 shows the geographical plot consisting of EQ locations and TC tracks between the JJI VLF transmitter and the two receiving stations; Vanuatu (left) and Fiji (right). The EQ on May 9, 2008 occurred during TC Rammasun and the EQ-related anomalies such as minimum nighttime and daytime amplitude, NF and wavelet spectrum of the perturbed signal were observed on the EQ day when the TC Rammasun was located outside the fifth Fresnel zone. Small perturbations in the night and day time amplitude and NF were also found when the TC in category 2–4 was located inside the sensitive zone. The EQ on 29 March which occurred during TC Jelawat has shown strong VLF anomalies a few days prior (NF, dispersion and WLS) and on the EQ day (variation in the signal amplitude, average nighttime amplitude, NF, and trend), before the TC was located inside the fifth Fresnel zone. On 30 March at 12 UT, the intensity of TC was maximum inside the sensitive zone, but only a few anomalies (NF and WLS) were seen. Also, before any VLF anomaly associated with this EQ was sensed, the tropical disturbance (TD) and TC Iris moved outside the wave sensitive zone. For the 16 November EQ, the EQ-related anomalies were sensed before the strengthening of TC Man_Yi, which formed TD on 20 November and later moved outside the wave sensitive zone. Thus, our analysis supports that the observed VLF anomalies are due to EQs during the period of these TCs. However, the EQ on August 21, 2018 which was located slightly beyond the fifth Fresnel zone did not show EQ-associated perturbations on the

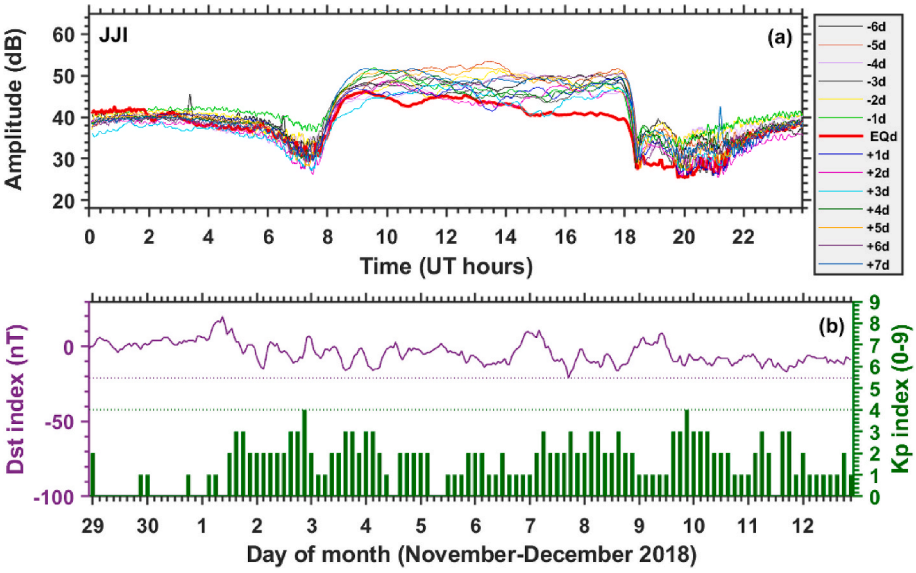

Fig. 8. (a) Diurnal variation in the signal amplitude of the JJI to Port Vila, Vanuatu, GCP for six days prior and seven days after the earthquake on December 5, 2018 with a magnitude of 7.5 and a depth of 10 km and (b) variation in the *Dst* and *Kp* indices for the days prior to and after the earthquake.

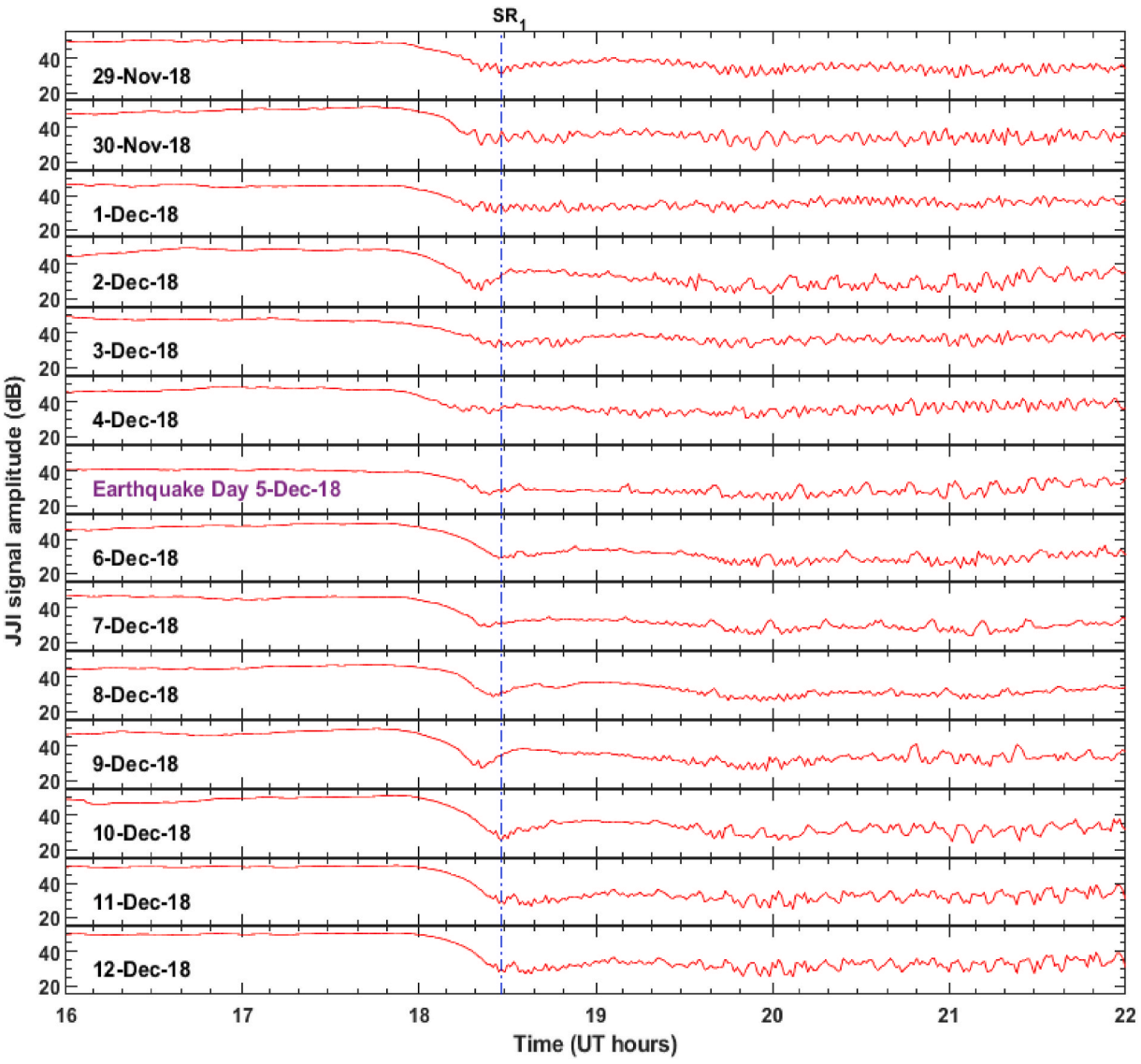

Fig. 9. Diurnal variation in the signal amplitude of the JJI to Port Vila, Vanuatu, during 29 November - December 12, 2018 associated with the earthquake on 5 December with a magnitude of 7.5 and a focus depth of 10 km. The horizontal axis represents the time in UT while the vertical axis in each panel shows the signal amplitude (dB). The dashed vertical line on the sunrise minima (SR_1) indicates the shift in terminator times.

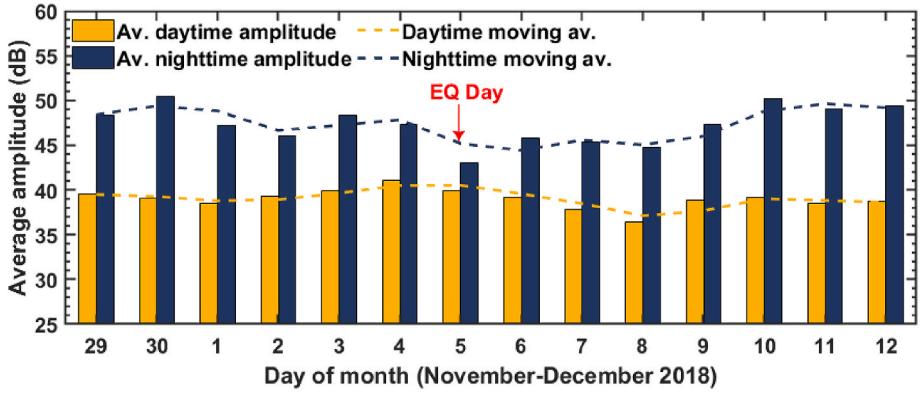

Fig. 10. The average amplitude during the daytime (23-06 UT hours) and at the nighttime (09–17 UT hours) of VLF signal for the JJI to Port Vila, Vanuatu path for a period of 29 November - December 12, 2018. The vertical red arrow on 5 December bar indicates the earthquake day. (For interpretation of the references to color in this figure legend, the reader is referred to the Web version of this article)

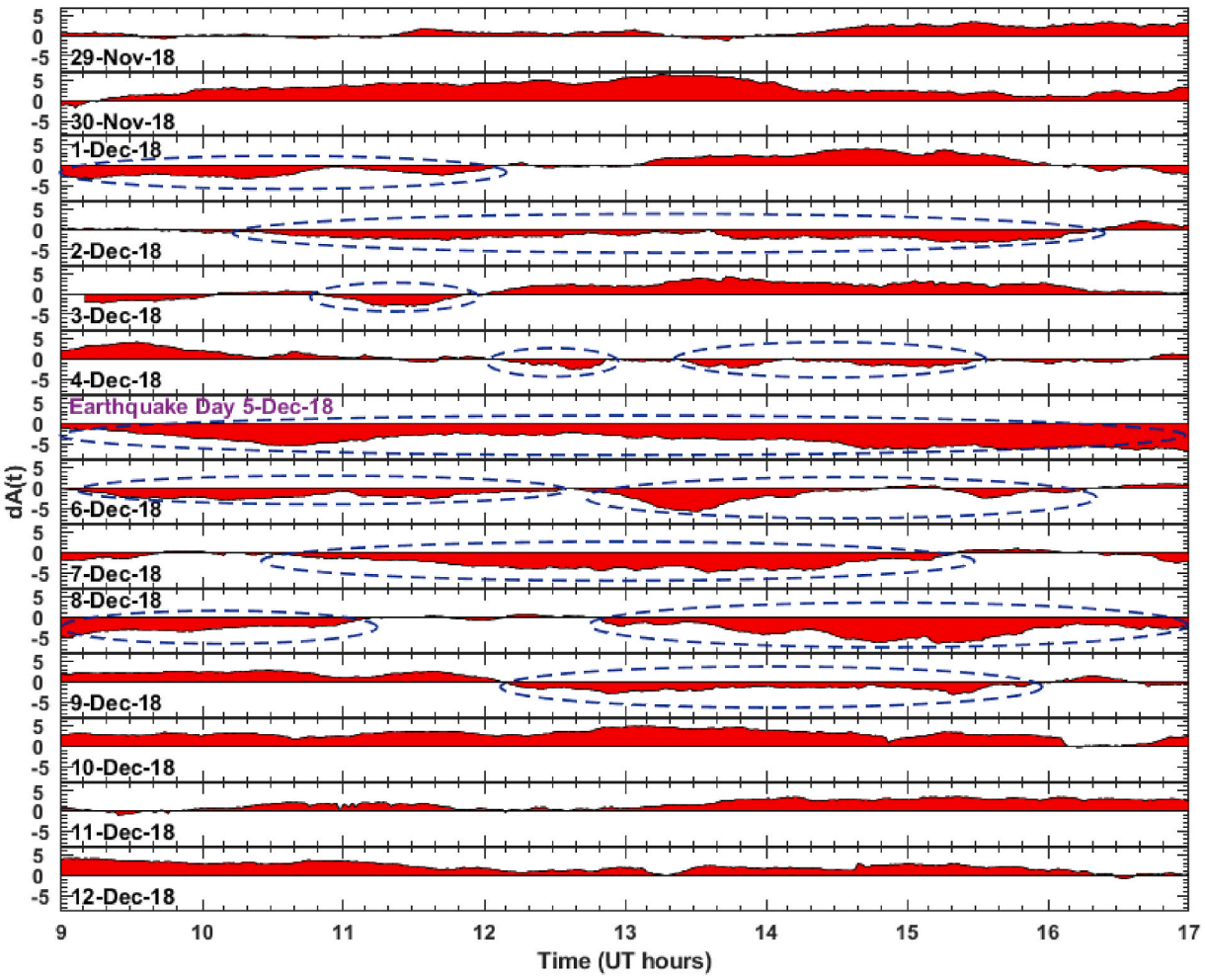

Fig. 11. Fluctuations in the nighttime signal strength (*y*-axis in dB) during 29 November - December 12, 2018 of the JJI to Port Vila, Vanuatu, GCP. The blue dashed ellipse indicates an increase in the occurrence of $dA(t) < 0$ conditions from 1 to 9 December. (For interpretation of the references to color in this figure legend, the reader is referred to the Web version of this article)

anomalous day (21 August) but marked most of the VLF perturbations (reduction in average daytime and nighttime amplitude, NF and WLS) from 16 to 23 August 2018.

A total of 11 EQs out of 16 have shown the VLF anomalies, two of which have been presented here as case studies. The first EQ on December 14, 2016 had its epicenter within the fifth Fresnel zone and the second EQ on December 5, 2018 had its epicenter located slightly beyond the fifth Fresnel zone which also showed EQ-related anomalies. Phanikumar et al. (2018) for EQs with the epicenter located outside the fifth Fresnel zone have reported VLF signal amplitude anomalies and the TTs shift. For the two EQs presented here, there were no TCs or space weather events present hence anomalies in VLF are attributed to purely EQ effects. For 7 EQs (4 EQs within the fifth Fresnel zone) with magnitude more than 5.5, maximum depth of 212 km, and maximum distance (~690 km) off the TRGCP, we found nighttime amplitude lower than the mean amplitude from 2 to 8 h on the EQ day. Three EQs with a magnitude more than 5.6, maximum depth of 34 km, EQ epicenter of ~6, 80, and 184 km away from the TRGCP showed a shift in the TTs. Under the normal conditions, the average shift for the 15 days in the time of occurrence of sunrise minima (SR_1) is 4 min which during these 3 EQs increased up to 5–9 min on the day of the EQ. TTs shift is due to an increase in the D-region electron density, which lowers the ionospheric boundary (Yoshida et al., 2008). The lowering of the D-region ionospheric boundary alters the conditions for the VLF modal interference (Maurya et al., 2016). Zhang et al. (2020) for Indonesian EQ on August 5, 2018 found that the nighttime ionospheric height around the EQ epicenter reduced from 26 July to 9 August to 85 km as compared to 95 km from 15 to 25 July.

Most of the EQs have not shown any significant shift(s) in the terminator time (TT) because the JJI-Port Vila propagation path is mainly in the north to south direction and fairly less in the west to the east direction to Suva. Clilverd et al. (1999) and Maekawa and Hayakawa (2006) have reported that N–S propagation itself is not appropriate for the detection of any TT effect. Kumar et al. (2013) for an EQ of magnitude 5.8 at a depth of 53 km within the fifth Fresnel zone reported a strong anomaly in the Indian VTX transmitter signal (18.2 kHz) received at Suva, Fiji, over the TRGCP length of 11.4 Mm. Their analysis yielded a shift in TT measuring up to ~20 min on the day of tremor.

In this work, for 9 EQs the average nighttime amplitude decreased from 1 to 5 dB and for 4 EQs average daytime amplitude reduced from ~1 to 1.5 dB. Kumar et al. (2008) suggested that reduced signal strength is due to higher attenuation of VLF propagation which depends on the reflection height of the VLF signal, where the higher VLF attenuation is generated by lowering the height of the EIWG (Kumar et al., 2008). From the EQ examined in our study, the nighttime fluctuation revealed that a total of 10 EQs showed significant $dA(t) < 0$ condition. These EQs had a magnitude of more than 5.5 with a depth of less than 212 km. In most cases, the $dA(t)$ values start to decrease about 4–5 days before the EQ event and stabilized after the EQ day (within 3–4 days after the event). These changes in the NF seem to indicate the upward

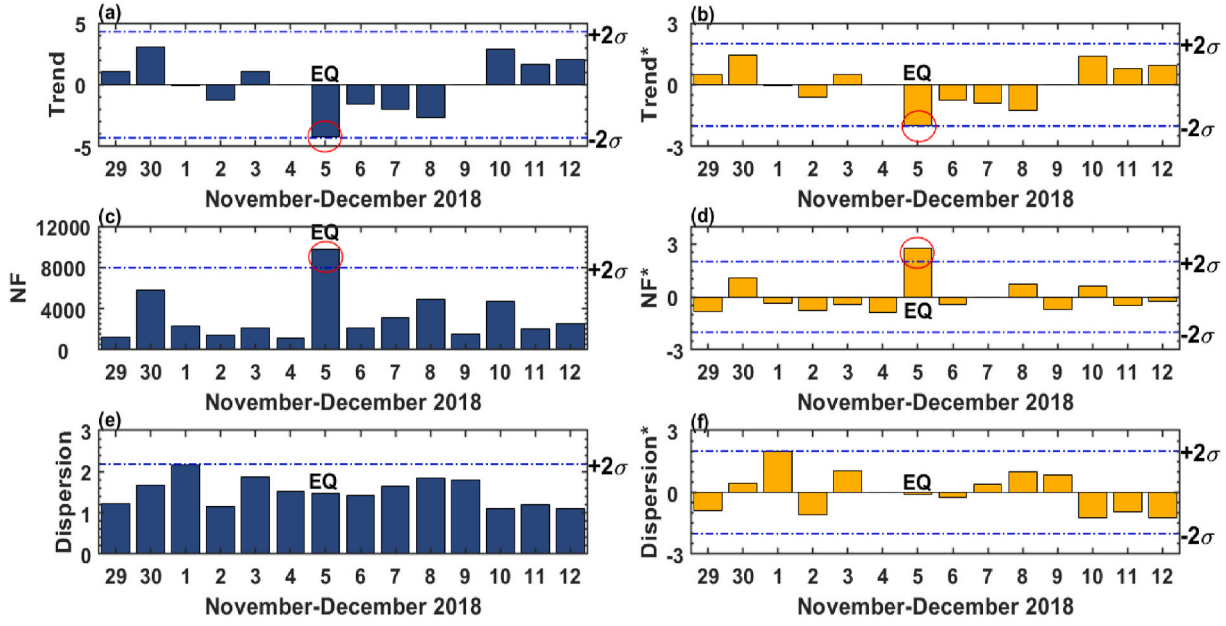

Fig. 12. Graphical representations of the trend (a), nighttime fluctuation (c), and dispersion (e) in each panel (left) during the period 29 November to December 12, 2018 for the JJI to Port Vila, Vanuatu, GCP. The panels (b, d and f) on the right side represent normalized values of the trend, NF, and dispersion. The blue horizontal dashed line shows the $\pm 2\sigma$ criterion. The red circle on the columns indicates anomalous values (crossing 2σ lines). (For interpretation of the references to color in this figure legend, the reader is referred to the Web version of this article)

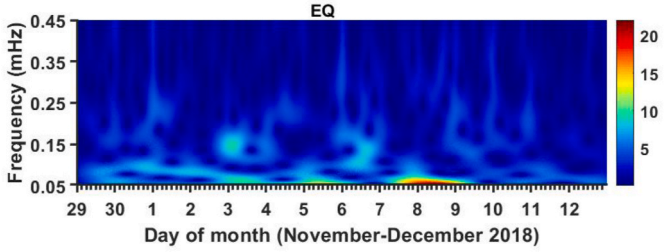

Fig. 13. The wavelet spectra of JJI VLF signal received at Port Vila, Vanuatu at the nighttime (09–17 UT hours) for the period 29 November to December 12, 2018. The earthquake day is 5 December.

propagating atmospheric gravity waves (AGWs) associated with EQs.

Three statistical parameters of VLF propagation, trend (T), nighttime fluctuation (NF) and dispersion (D) are widely used in EQ analysis where the anomaly is considered by the simultaneous decrease in the T and rise in the NF and D (Hayakawa et al., 2010; Kumar et al., 2013). From our analysis for 16 EQs, only 3 EQs displayed a decrease in the non-normalized and normalized T before the EQ day and moved below the -2σ mark on the EQ day, and an increase in the non-normalized and normalized NF and D before the EQ day reached above the +2σ mark on the EQ day. These anomalies were observed for EQs with magnitude more than 5.5, shallow depth up to 32 km, and epicenter position less than 185 km off the TRGCP. Our results are consistent with the earlier results of Hayakawa et al. (2011), Kasahara et al. (2010) and Khadka et al. (2017) who found a simultaneous decrease in the T and increase in the NF and D. The T showed a decrease in the average of nighttime $dA(t)$ values on EQ day because of the reduction in the ionospheric VLF

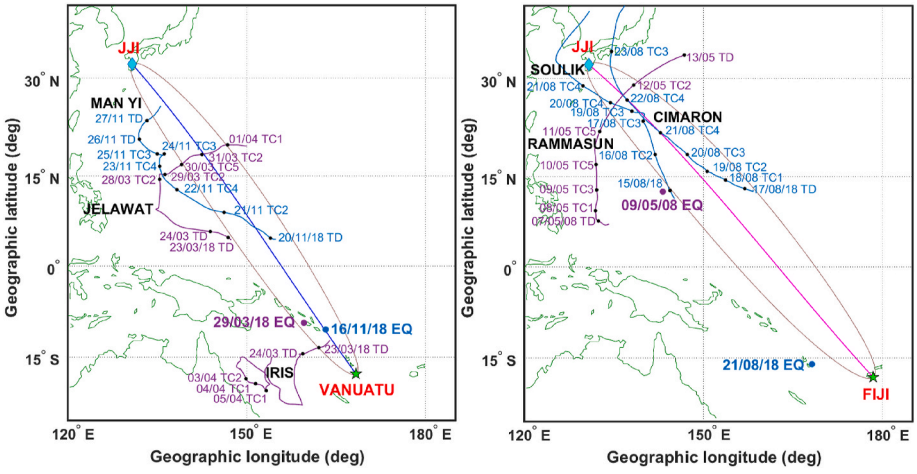

Fig. 14. The location of the earthquakes, tracks of tropical cyclones, great circle path between the JJI VLF transmitter and the two receiving stations; Vanuatu (left) and Fiji (right). The wave sensitive area (fifth Fresnel zone) is plotted with the brown ellipse. (For interpretation of the references to color in this figure legend, the reader is referred to the Web version of this article)

reference height (Molchanov et al., 1998; Zhao et al., 2020).

The AGWs act as a carrier for the tropospheric disturbances to the ionosphere (Pal et al., 2020). Here, the mother Morlet wavelet (Mallat, 1999) technique was used to estimate the frequencies of the wave-like signatures (WLS) in the EQ-associated VLF signal perturbations associated with AGWs. Researchers have also carried out the Wavelet analysis of the difference $dA(t)$ and computed the spectral intensity of the VLF fluctuations due to EQs (Hayakawa, 2007; Sánchez-Dulcet et al., 2015). Based on our results, 7 EQs revealed the wavelet signals of a short frequency (~0.05–0.10 mHz) on pre-EQ, co-EQ, and post-EQ days. This short frequency range indicates nighttime WLS for the durations of 2.7 and 5.5 h for EQs with a magnitude more than 5.5 and a focus depth less than 184 km. Horie et al. (2007) considered VLF signal from the NWC transmitter (19.8 kHz) at the three Japanese stations (Chofu, Chiba, and Kochi) to identify any possible ionospheric anomalies associated with the huge Sumatra EQ ($Mw = 9.3$) on December 26, 2004. Their results showed significant enhancement in wave-like spectra of period 20–30 min to about 100 min (the frequency range of AGWs) only before the EQ.

The presence of pre-EQ ionospheric variation and their possible genesis have been discussed (Oikonomou et al., 2016; Pulinets et al., 1998), but the linkage between the lithosphere, atmosphere and ionosphere for the duration of the seismic events are still not completely understood and are a topic of scientific controversy and debate which warrants further analyses such as presented in this paper. The three channels that are proposed to link the EQ preparatory occurrence with the ionosphere are; (1) chemical (2) wave channel (including acoustic gravity waves) and (3) electromagnetic channel which is connected with the vertical electric field that propagates to the ionosphere (Liu et al., 2001). The first channel is associated with the geochemical effect, which causes ionospheric modification through the atmospheric electric field. The second channel is due to atmospheric oscillations induced in the EQ-active region which can move up to the ionosphere. The third channel is supposed to be inadequate due to the weak intensity of radio emissions produced in the EQ preparatory zone (Hayakawa and Molchanov, 2004; Hayakawa et al., 2004). The modification of the atmospheric electric field by the geo-electric field generated by the piezo-electric field in the seismic sensitive zone may play a vital part in the lithosphere-atmosphere-ionosphere coupling (Kelley et al., 2017; Pulinets and Ouzounov, 2011). The induced EQ vertical electric field of 1000 mV/m at a height more than 60 km over EQ active region a few days before the seismic activity penetrates the ionosphere and perturbs the ionospheric electrodynamics and the electron density by changing the F-region $\mathbf{E} \times \mathbf{B}$ plasma drifts (Pulinets et al., 1998). The lower ionosphere can be perturbed due to the coupling of the lower ionosphere with the upper ionosphere (Ohya et al., 2006; Maurya et al., 2022).

During the active or preparatory EQ times, the release of radon and other gases (electrochemical processes) in addition to piezo-electric effects may penetrate the lower ionosphere and change its conductivity. Molchanov (1991) suggested that the broad-band electromagnetic (EM) emissions are generated during the movement and destruction of blocks of the earth's core along the sensitive cracks near the center of an EQ preparatory zone. The excitation of acoustic GWs may result from the production of non-stationary Joule heating (Heki, 2011; Kim and Nikiforova, 1997). These AGWs on propagating into the ionosphere cause the neutral densities of the mesosphere and lower thermosphere to lift and sink affecting the lithosphere-atmosphere-ionosphere (LAI) coupling. The AGWs generated Rayliegh-Taylor instability may travel a greater distance (a few 1000 km) from the epicenter (Liperovskaya et al., 1994; Shalimov and Gokhberg, 1998). Researchers (Mareev, 2002; Molchanov, 2004) have suggested that AGWs action is effective at smaller distances from the epicenter because of mosaic-like structure. Few models of LAI coupling considered the alteration of the atmospheric electric field by the increase in radioactivity and electrical conductivity (Pulinets et al., 1997; Sorokin, 1999). Another modification to LAI coupling is through quasi-electrostatic field which involves the discharge of radon gas into the Earth's atmosphere from the EQ preparation zone (Pulinets and Boyarchuk, 2004; Pulinets et al., 1998, 2000). However, the wavelet analysis of VLF signal perturbation events presented in this study provides an evidence for the D-region perturbations associated with EQs. The propagation of AGWs to the D-region can be altered by background wind (Cowling et al., 1971) which at times may not be favorable for AGWs reaching D-region and hence AGWs were not detected for all EQs.

5. Conclusions

Subionospheric JJI VLF transmitter signal recorded at two low-latitude stations during 2007–2018 due to 16 EQ events has been studied. The findings of the study are concluded as follows:

- The nighttime signal amplitude for 7 EQs (4 EQs within the fifth Fresnel zone) reduced to a lower level than the mean amplitude for approximately more than 2–8 h during the EQ day.
- Three EQs with a magnitude more than 5.6, maximum focus depth of 34 km, the epicenter of ~6, 80, and 184 km off the TRGCP showed shifts in the TTs of up to 5–9 min on the EQ day as compared to the normal shift of about 4 min.
- A decrease in the average nighttime amplitude on the EQ day was found for 9 EQ events in which the amplitude decreased about 1–5 dB while only 4 EQs were noticed to have average daytime amplitude reduced on the EQ day (reduced amplitude of ~1–1.5 dB) which is due to a decrease in the D-region VLF reflection height.
- The nighttime fluctuation revealed that a total of 10 EQs showed significant $dA(t) < 0$ condition. These EQs had a magnitude of more than 5.5 and a depth of less than 212 km. In most cases, the $dA(t)$ decreased about 4–5 days before the EQ and stabilized after the EQ day (within 3–4 days after the event) indicating the signatures of AGWs revealed by Wavelet analysis of the perturbed signal.
- Three EQs showed a decrease in the non-normalized and normalized trend before the EQ day below the -2σ mark on the EQ day. The increase in the non-normalized and normalized NF and dispersion was found before the EQ day above the +2σ mark on the EQ day. These anomalies were observed for EQs with a magnitude more than 5.5, shallow depth up to 32 km, and epicenter position less than 185 km off the TRGCP.
- Seven EQs showed the Wavelet spectrum of the short frequency range (~0.05–0.10 mHz) on pre-, co-, and post-EQ times. The stronger nighttime wave-like signatures for the durations from 2.7 to 5.5 h as compared to normal days were observed for EQs with the magnitude more than 5.5 and the fucus depth less than 184 km.

Funding

The University of the South Pacific, Suva, Fiji.

Data availability

The Dst and K_P indices data were obtained from the World Data Center, Kyoto University, Kyoto, Japan (online at http://wdc.kugi.kyoto-u.ac.jp/wdc/Sec3.html) and the solar flare data was obtained from the SpaceWeatherLive.com (https://www.spaceweatherlive.com/en/solar-activity/solar-flares.html). The data sets used in this research for TCs are from NOAA (IBTrACS) https://www.ncdc.noaa.gov/ibtracs/.

Declaration of competing interest

The authors declare that they have no known competing financial interests or personal relationships that could have appeared to influence the work reported in this paper.

Acknowledgments

The authors are also thankful for the financial support by The University of the South Pacific's main research office under the Strategic Research Theme (Grant No. F7304-RI001-ACC-001) under which this work has been carried out.

References

Astafyeva, E., Shalimov, S., Olshanskaya, E., Lognonné, P., 2013. Ionospheric response to earthquakes of different magnitudes: larger quakes perturb the ionosphere stronger and longer. Geophys. Res. Lett. 40 (9), 1675–1681. https://doi.org/10.1002/grl.50398.

Clilverd, M.A., Thomson, N.R., Rodger, C.J., 1999. Sunrise effects on VLF signals propagating over a long north-south path. Radio Sci. 34 (4), 939–948. https://doi.org/10.1029/1999RS900052.

Cowling, D.H., Webb, H.D., Yeh, C.K., 1971. Group rays of internal gravity waves in a wind-stratified atmosphere. J. Geophys. Res. 76, 200–213. https://doi.org/10.1029/JA076i001p00213.

Freund, F., 2013. Earthquake forewarning - a multidisciplinary challenge from the ground up to space. Acta Geophys. 61 (4), 775–807. https://doi.org/10.2478/s11600-013-0130-4.

Hayakawa, M., 2007. VLF/LF radio sounding of ionospheric perturbations associated with earthquakes. Sensors 7 (7), 1141–1158. https://doi.org/10.3390/s7071141.

Hayakawa, M., Raulin, J., Kasahara, Y., Bertoni, F., Hobara, Y., Guevara-Day, W., 2011. Ionospheric perturbations in possible association with the 2010 Haiti earthquake, as based on medium-distance subionospheric VLF propagation data. Nat. Hazards Earth Syst. Sci. 11 (2), 513. https://doi.org/10.5194/nhess-11-513-2011.

Hayakawa, M., Molchanov, O., 2004. Summary report of NASDA's earthquake remote sensing frontier project. Phys. Chem. Earth, Parts A/B/C 29 (4–9), 617–625. https://doi.org/10.1016/j.pce.2003.08.062.

Hayakawa, M., Molchanov, O., Team, N.U., 2004. Achievements of NASDA's Earthquake Remote Sensing Frontier Project. https://doi.org/10.3319/TAO.2004.15.3.311(EP).

Hayakawa, M., Kasahara, Y., Nakamura, T., Muto, F., Horie, T., Maekawa, S., Hobara, Y., Rozhnoi, A., Solovieva, M., Molchanov, O.A., 2010. A statistical study on the correlation between lower ionospheric perturbations as seen by subionospheric VLF/LF propagation and earthquakes. J. Geophys. Res.: Space Physics 115 (A9). https://doi.org/10.1029/2009JA015143.

Heki, K., 2011. Ionospheric electron enhancement preceding the 2011 Tohoku-Oki earthquake. Geophys. Res. Lett. 38 (17) https://doi.org/10.1029/2011GL047908.

Horie, T., Yamauchi, T., Yoshida, M., Hayakawa, M., 2007. The wave-like structures of ionospheric perturbation associated with Sumatra earthquake of 26 December 2004, as revealed from VLF observation in Japan of NWC signals. J. Atmos. Sol. Terr. Phys. 69 (9), 1021–1028. https://doi.org/10.1016/j.jastp.2007.03.012.

Kakinami, Y., Kamogawa, M., Onishi, T., Mochizuki, K., Lebreton, J.-P., Watanabe, S., Yamamoto, M.-Y., Mogi, T., 2013. Validation of electron density and temperature observed by DEMETER. Adv. Space Res. 52 (7), 1267–1273. https://doi.org/10.1016/j.asr.2013.07.003.

Kasahara, Y., Muto, F., Hobara, Y., Hayakawa, M., 2010. The ionospheric perturbations associated with Asian earthquakes as seen from the subionospheric propagation from NWC to Japanese stations. Nat. Hazards Earth Syst. Sci. 10 (3), 581. https://doi.org/10.5194/nhess-10-581-2010.

Kelley, M.C., Swartz, W.E., Heki, K., 2017. Apparent ionospheric total electron content variations prior to major earthquakes due to electric fields created by tectonic stresses. J. Geophys. Res.: Space Physics 122 (6), 6689–6695. https://doi.org/10.1002/2016JA023601.

Kerrache, F., Nait Amor, S., Kumar, S., 2021. Ionospheric D region disturbances due to FAC and LEP associated with three severe geomagnetic storms as observed by VLF signals. J. Geophys. Res.: Space Physics 126, e2020JA027838. https://doi.org/10.1029/2020JA027838.

Khadka, B., Kandel, K.P., Pant, S., Bhatta, K., Ghimire, B.D., 2017. VLF/LF amplitude perturbations before tuscany earthquakes. Nat. Sci. 9 (12), 437. https://doi.org/10.4236/ns.2017.912041, 2013.

Kim, V., Nikiforova, L., 1997. A possible generation mechanism of acoustic-gravity waves in the ionosphere before strong earthquakes. Journal of Earthquake Prediction Research 6, 584–589.

Kumar, A., Kumar, S., Hayakawa, M., Menk, F., 2013. Subionospheric VLF perturbations observed at low latitude associated with earthquake from Indonesia region. J. Atmos. Sol. Terr. Phys. 102, 71–80. https://doi.org/10.1016/j.jastp.2013.04.011.

Kumar, S., Kumar, A., Rodger, C., 2008. Subionospheric early VLF perturbations observed at Suva: VLF detection of red sprites in the day? J. Geophys. Res.: Space Physics 113 (A3). https://doi.org/10.1029/2007JA012734.

Kumar, S., Kumar, A., Menk, F., Maurya, A.K., Singh, R., Veenadhari, B., 2015. Response of the low-latitude D-region ionosphere to extreme space weather event of 14–16 December 2006. J. Geophys. Res.: Space Physics 120, 788–799. https://doi.org/10.1002/2014JA020751.

Kumar, S., NaitAmor, S., Chanrion, O., Neubert, T., 2017. Perturbations to the lower ionosphere by tropical cyclone Evan in the South Pacific region. J. Geophys. Res.: Space Physics 122, 8720–8732. https://doi.org/10.1002/2017JA024023.

Liperovskaya, E., Hristakis, N., Liperovsky, V., Oleinik, M., 1994. Effects of seismic and anthropogenic activity in the nighttime sporadic ionospheric E layer. Geomagn. Aeron. 34 (3), 56–59.

Liu, J., Chen, Y., Chuo, Y., Tsai, H., 2001. Variations of ionospheric total electron content during the Chi-Chi earthquake. Geophys. Res. Lett. 28 (7), 1383–1386. https://doi.org/10.1029/2000GL012511.

Maekawa, S., Hayakawa, M., 2006. A statistical study on the dependence of characteristics of VLF/LF terminator times on the propagation direction. IEEJ Transactions on Fundamentals and Materials 126 (4), 220–226. https://doi.org/10.1541/ieejfms.126.220.

Mallat, S., 1999. A Wavelet Tour of Signal Processing. Elsevier. https://doi.org/10.1016/B978-0-12-374370-1.X0001-8.

Mareev, E., 2002. Mosaic source of internal gravity waves associated with seismic activity. Seismo-Electromagnetics: Lithosphere-Atmosphere–Ionosphere Coupling 335–343.

Maurya, A.K., Venkatesham, K., Tiwari, P., Vijaykumar, K., Singh, R., Singh, A.K., Ramesh, D., 2016. The 25 April 2015 Nepal Earthquake: investigation of precursor in VLF subionospheric signal, 10 J. Geophys. Res.: Space Physics 121 (10), 403–410. https://doi.org/10.1002/2016JA022721, 416.

Maurya, A.K., Parihar, N., Dube, A., Singh, R., Kumar, S., Chanrion, O., Tomicic, M., Neubert, T., 2022. Rare observations of sprites and gravity waves supporting D, E,F-regions ionospheric coupling. Scientifc Reports 12, 58. https://doi.org/10.1038/s41598-021-03808-5.

Molchanov, O.A., 1991. Propagation of electromagnetic fields from seismic sources into the upper ionosphere. Geomagn. Aeron. 31, 111–119.

Molchanov, O.A., 2004. On the origin of low-and middler-latitude ionospheric turbulence. Phys. Chem. Earth, Parts A/B/C 29 (4–9), 559–567. https://doi.org/10.1016/j.pce.2003.11.018.

Molchanov, O.A., Hayakawa, M., Oudoh, T., Kawai, E., 1998. Precursory effects in the subionospheric VLF signals for the Kobe earthquake. Phys. Earth Planet. In. 105 (3–4), 239–248. https://doi.org/10.1016/S0031-9201(97)00095-2.

Němec, F., Santolík, O., Parrot, M., Berthelier, J.-J., 2008. Spacecraft observations of electromagnetic perturbations connected with seismic activity. Geophys. Res. Lett. 35 (5) https://doi.org/10.1029/2007GL032517.

Nina, A., Biagi, P.F., Mitrović, S.T., Pulinets, S., Nico, G., Radovanović, M., Popović, L.Č., 2021. Reduction of the VLF signal phase noise before earthquakes. Atmosphere 12 (4), 444. https://doi.org/10.3390/atmos12040444.

Oikonomou, C., Haralambous, H., Musoim, B., 2016. Investigation of ionospheric TEC precursors related to the M7. 8 Nepal and M8. 3 Chile earthquakes in 2015 based on spectral and statistical analysis. Nat. Hazards 83 (1), 97–116. https://doi.org/10.1007/s11069-016-2409-7.

Ohya, H., Nishino, M., Murayama, Y., Igarashi, K., Saito, A., 2006. Using tweek atmospherics to measure the response of the low-middle latitude D-region ionosphere to a magnetic storm. J. Atmos. Sol. Terr. Phys. 68 (6), 697–709. https://doi.org/10.1016/j.jastp.2005.10.014.

Pal, S., Sarkar, S., Midya, S.K., Mondal, S.K., Hobara, Y., 2020. Low-latitude VLF radio signal disturbances due to the extremely severe cyclone fani of may 2019 and associated mesospheric response. J. Geophys. Res.: Space Physics 125 (5), e2019JA027288. https://doi.org/10.1029/2019JA027288.

Phanikumar, D., Maurya, A.K., Kumar, K.N., Venkatesham, K., Singh, R., Sharma, S., Naja, M., 2018. Anomalous variations of VLF sub-ionospheric signal and mesospheric ozone prior to 2015 gorkha Nepal earthquake. Sci. Rep. 8 (1), 1–9. https://doi.org/10.1038/s41598-018-27659-9.

Pulinets, S., Legen'ka, A., Zelenova, T., Aeronomy, 1998. Local-time dependence of seismo-ionospheric variations at the F-layer maximum. Geomagn. Aeron. 38 (3), 400–402.

Pulinets, S., Ouzounov, D., 2011. Lithosphere–Atmosphere–Ionosphere Coupling (LAIC) model–An unified concept for earthquake precursors validation. J. Asian Earth Sci. 41 (4–5), 371–382. https://doi.org/10.1016/j.jseaes.2010.03.005.

Pulinets, S., Boyarchuk, K., 2004. Ionospheric Precursors of Earthquakes. Springer Science & Business Media. https://doi.org/10.1007/b137616.

Pulinets, S., Boyarchuk, K., Hegai, V., Kim, V., Lomonosov, A., 2000. Quasielectrostatic model of atmosphere-thermosphere-ionosphere coupling. Adv. Space Res. 26 (8), 1209–1218. https://doi.org/10.1016/S0273-1177(99)01223-5.

Pulinets, S., Alekseev, V., Legen'ka, A., Khegai, V., 1997. Radon and metallic aerosols emanation before strong earthquakes and their role in atmosphere and ionosphere modification. Adv. Space Res. 20 (11), 2173–2176. https://doi.org/10.1016/S0273-1177(97)00666-2.

Righetti, F., Biagi, F., Maggipinto, T., Schiavulli, L., Ligonzo, T., Ermini, A., Moldovan, I. A., Moldovan, A.S., Buyuksarac, A., Silva, H.G., 2012. Wavelet Analysis of the LF Radio Signals Collected by the European VLF/LF Network from July 2009 to April 2011, *Annals Of Geophysics*. https://doi.org/10.4401/ag-5188.

Rodger, C.J., 2003. Subionospheric VLF perturbations associated with lightning discharges. J. Atmos. Sol. Terr. Phys. 65 (5), 591–606. https://doi.org/10.1016/S1364-6826(02)00325-5.

Salut, M.M., Abdullah, M., Graf, K.L., Cohen, M.B., Cotts, B.R.T., Kumar, S., 2012. Long recovery VLF perturbations associated with lightning discharges. J. Geophys. Res. 117, A08311. https://doi.org/10.1029/2012JA017567.

Salut, M.M., Cohen, M.B., Ali, M.A.M., Graf, K.L., Cotts, B.R.T., Kumar, S., 2013. On the relationship between lightning peak current and early VLF perturbations. J. Geophys. Res.: Space Physics 118. https://doi.org/10.1002/2013JA019087.

Sánchez-Dulcet, F., Rodríguez-Bouza, M., Silva, H.G., Herraiz, M., Bezzeghoud, M., Biagi, P., 2015. Analysis of observations backing up the existence of VLF and ionospheric TEC anomalies before the Mw6. 1 earthquake in Greece. January 26, 2014, Physics and Chemistry of the Earth, Parts A/B/C 85, 150–166. https://doi.org/10.1016/j.pce.2015.07.002.

Selvakumaran, R., K Maurya, A., Gokani, S.A., Veenadhari, B., Kumar, S., Phanikumar, K. Venkatesham D., Singh, A.K., Siingh, D., Singh, R., 2015. Solar flares induced D-

region ionospheric and geomagnetic perturbations. J. Atmos. Sol. Terr. Phys. 123, 102–112. https://doi.org/10.1016/j.jastp.2014.12.009.

Shalimov, S., Gokhberg, M., 1998. Lithosphere–ionosphere coupling mechanism and its application to the earthquake in Iran on June 20, 1990. A review of ionospheric measurements and basic assumptions. Phys. Earth Planet. In. 105 (3–4), 211–218. https://doi.org/10.1016/S0031-9201(97)00092-7.

Silva, H.G., Bezzeghoud, M., Reis, A., Rosa, R., Tlemçani, M., Araújo, A., Serrano, C., Borges, J., Caldeira, B., Biagi, P., 2011. Atmospheric electrical field decrease during the M= 4.1 Sousel earthquake (Portugal). Nat. Hazards Earth Syst. Sci. 11 (3), 987. https://doi.org/10.5194/nhess-11-987-2011.

Silva, H.G., Bezzeghoud, M., Oliveira, M.M., Reis, A.H., Rosa, R.N., 2013. A simple statistical procedure for the analysis of radon anomalies associated with seismic activity. Ann. Geophys. 56 (1), 0106, 10.4401/ag-5570.

Sorokin, V., 1999. Modification of the Ionosphere by Seismic Related Electric Field, *Atmospheric And Ionospheric Electromagnetic Phenomena Associated With Earthquakes*, pp. 805–818.

Yoshida, M., Yamauchi, T., Horie, T., Hayakawa, M., 2008. On the generation mechanism of terminator times in subionospheric VLF/LF propagation and its possible application to seismogenic effects. Nat. Hazards Earth Syst. Sci. 8 (1), 129–134. https://doi.org/10.5194/nhess-8-129-2008.

Zhang, X., Wang, Y., Boudjada, M.Y., Liu, J., Magnes, W., Zhou, Y., Du, X., 2020. Multi-experiment observations of ionospheric disturbances as precursory effects of the Indonesian Ms6. 9 earthquake on August 05, 2018. Rem. Sens. 12 (24), 4050. https://doi.org/10.3390/rs12244050.

Zhao, S., Shen, X., Liao, L., Zhima, Z., Zhou, C., Wang, Z., Cui, J., Lu, H., 2020. Investigation of precursors in VLF subionospheric signals related to strong earthquakes (M> 7) in western China and possible explanations. Rem. Sens. 12 (21), 3563. https://doi.org/10.3390/rs12213563.